0209 Proceedings of the Japan Society of Mechanical Engineers
17th Computational Mechanics Conference, Sendai, Japan (2004).
17 回計算力学講演会・2004/11/18-20

ソロバン格子を用いた流体計算

Flow Calculations with the Soroban CIP Scheme

滝沢　研二・東京工業大学

Kenji Takizawa, Tokyo Institute of Technology

矢部　孝・東京工業大学

Takashi Yabe, Tokyo Institute of Technology

Tayfun E. Tezduyar・Rice University

Tayfun E. Tezduyar, Rice University

Key Words: *CFD, Boundary Layer, semi-Lagrangian CIP, CCUP, Grid generation*

1. INTRODUCTION

In recent years, with improved computing environments, demand for high-accuracy numerical methods has been rapidly increasing for various applications of fluid mechanics. Unstructured grids can represent the detailed flow patterns like the boundary layers around complex bodies [1]. However, it is known that coordinate transformation results in loss of accuracy in CIP calculations [2]. A “Soroban grid” allows accurate computations with unstructured grid functionality. With that, we can use the CIP method [3-5], which is third-order accurate on Soroban grids, and be able to use grids that can capture the boundary layers.

2. GRID GENERATION

2.1 GRID SYSTEM

A Soroban grid is composed of lines and grid points as shown in Fig. 1. Each line is set parallel to the x axis, but its y position is free, and each grid point along a line can be positioned freely.

2.2 GRID GENERATION AROUND OBJECTS

New grid positions are determined from the following equation:

$$\int_{x_S}^{x_k^{n+1}} M(x,t)\,dx = \frac{k}{N}\int_{x_S}^{x_E} M(x,t)\,dx \quad , \tag{1}$$

where M is a monitoring function, N is the number of grid points in the section from x_S to x_E, and k is the grid point counter. In order to represent the boundary, x_S and x_E are determined using a distance function. Then the grid generation is performed as follows:

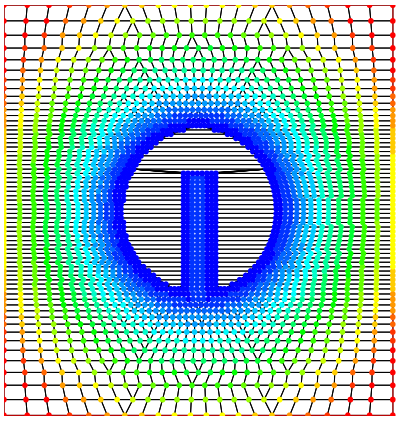

Figure 1 Soroban grid generated by distance function around objects.

i) Calculate the distance function $D(x,y,t)$,
ii) Search $D(x,y,t)=0$ for x_S and x_E,
iii) Calculate M in each section,
iv) Calculate new grid position x.

The monitoring functions for Fig. 1 are given as:

$$M(x,t) = \frac{1}{\Delta x + D(x,y,t)} \quad , \tag{2}$$

where Δx is the minimum grid spacing in x direction, and

$$M(y,t) = Max\left(\frac{1}{\Delta y + \kappa\left|\partial D/\partial y\right| + D}\right) \quad , \tag{3}$$

where the Max function selects the maximum value of its argument along the x direction, κ is a pre-determined coefficient, and Δy is the minimum grid spacing in y direction.

3. NUMERICAL FORMULATION

In the CCUP [6-7] method, the governing equations are given as follows:

$$\frac{\partial \boldsymbol{u}}{\partial t} + \boldsymbol{u}\cdot\nabla\boldsymbol{u} = -\frac{1}{\rho}\nabla p + \nu\nabla^2\boldsymbol{u} \quad , \tag{4}$$

$$\frac{\partial p}{\partial t} + \boldsymbol{u}\cdot\nabla p = -\rho Cs\,\nabla\cdot\boldsymbol{u} \quad , \tag{5}$$

where Cs is the local speed of sound and ν is the kinematic viscosity.
These equations are divided into three parts in a fractional step method:

i) Non-Advection Part 1

$$\frac{\boldsymbol{u}^{NA1}-\boldsymbol{u}^{n}}{\Delta t} = \nu\nabla^2\boldsymbol{u}^{NA1} \quad , \tag{6}$$

ii) Non-Advection Part 2

$$\frac{p^{NA2}-p^{n}}{\rho Cs(\Delta t)^2} - \frac{\nabla\cdot\boldsymbol{u}^{NA1}}{\Delta t} = -\nabla\cdot\left(\frac{1}{\rho}\nabla p^{NA2}\right) \quad , \tag{7}$$

$$\frac{\boldsymbol{u}^{NA2}-\boldsymbol{u}^{NA1}}{\Delta t} = -\frac{1}{\rho}\nabla p^{NA2} \quad . \tag{8}$$

iii) Mesh update and Advection

Update the mesh using the monitoring functions defined.
Then,

$$\phi^{n}_{new} = \phi^{NA2}_{old}\left(\boldsymbol{x}_{new} - \bar{\boldsymbol{u}}\Delta t\right) \quad , \tag{9}$$

where, ϕ is replaced by $\boldsymbol{u}$ and p, subscript "new" means the new grid, "old" means the old grid, and the velocity is calculated as follows:

$$\bar{\boldsymbol{u}} = \frac{\boldsymbol{u}_{old}^{NA2}(x_{new}) + \boldsymbol{u}_{new}^{NA2}\left(x_{new} - \boldsymbol{u}_{old}^{NA2}(x_{new})\Delta t\right)}{2} \quad . \tag{10}$$

This velocity calculation is based on the method given in [2], to increase the accuracy in locating the upwind point. The calculations are carried out by using the CIP method.

4. FLOW PAST A CIRCULAR CYLINDER

The Reynolds number is 100, and at this Reynolds number we have Karman vortex shedding. We compare the results to those reported in [8]. The dimensions of the computational domain are 60x16 (normalized by the cylinder diameter), and the cylinder is located at (8, 8). The Soroban lines are parallel to the y axis, and the grid points are located on each line in a way to refine the grid where it is needed.

We switch the monitoring function depending on the distance from the surface. If D < 3 diameters, we use Eqs. (2) and (3), otherwise we use a single monitoring function:

$$M(x,y,t) = \frac{1}{\Delta x}\left(1 + \alpha\left|\frac{\partial u}{\partial y} - \frac{\partial v}{\partial x}\right|\right) \quad . \tag{11}$$

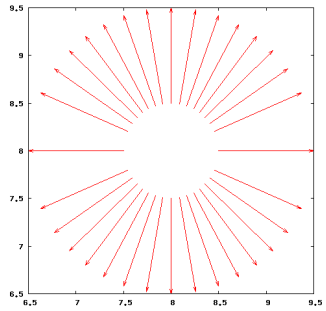

Figure 2 Grid points and normal vectors around a circular cylinder.

As seen in Fig. 2, about 32 grid points are on the cylinder surface.

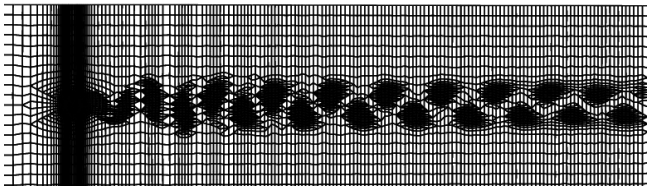

Figure 3 Grid points at an instant during computation. Grid lines are for visialization only.

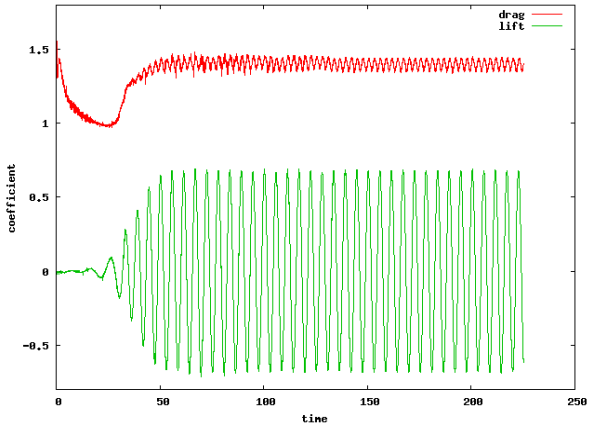

Figure 4 Drag and lift coefficients.

The computed Strouhal number is 0.173, and the drag coefficient is 1.40. These result are reasonably close to the results reported in [8]. A long wake of vortex shedding is seen in this problem. Because this is an advection dominated phenomenon, it is calculated with the CIP method accurately, as seen in Figs. 3-5.

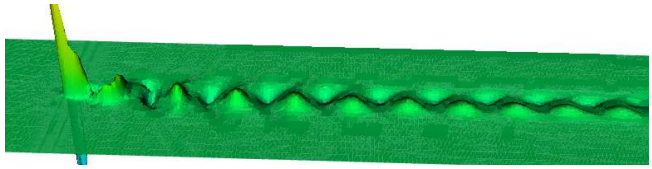

Figure 5 Vorticitiy.

5. CONCLUSION

In the context of computation of incompressible flows, we have developed a CIP technique based on Soroban grid generation with refinement control near solid surfaces. By using a semi-Lagrangian CIP technique and by treating the viscous terms implicitly we remove to a large extent the times-step size limitations. Our grid generation is based on a level set approach and gives us extensive control of the mesh resolution in the boundary layers. In addition, our grid generation is solution-adaptive, and with that high refinement zones follow the advected vortices. The grid refinement in boundary layers is not as effective as it is with, for example, a finite element approach, yet the results are in reasonably good agreement with those obtained from finite element computations [8]. Although we have presented this method in the context of incompressible flows, the underlying numerical technique, the CCUP method, is also applicable to compressible flows. With the steps taken in this paper, the CCUP method becomes closer to being a general-purpose flow computation technique.

REFERENCE

[1] T.E. Tezduyar, Finite element methods for flow problems with moving boundaries and interfaces, Arch. Comput. Methods Eng. 8 (2001) 83.

[2] T. Yabe, et al. Higher-order schemes with CIP method and adaptive Soroban grid towards mesh-free scheme, Journal of Computational Physics 194 (2004) 57.

[3] H. Takewaki, A. Nishiguchi, T. Yabe, The cubic-interpolated pseudo-particle (CIP) method for solving hyperbolic-type equations, J. Comput. Phys. 70 (1985) 261.

[4] H. Takewaki, T. Yabe, Cubic-interpolated pseudo particle (CIP) method - application to nonlinear or multi-dimensional problems, J. Comput. Phys. 70 (1987) 355.

[5] T. Aoki, Multi-dimensional advection of CIP (cubic-interpolate propagation) scheme, CFD J. 4 (1995) 279.

[6] T. Yabe, P.Y. Wang, Unified numerical procedure for compressible and incompressible fluid, J. Phys. Soc. Jpn. 60 (1991) 2105.

[7] S.Y. Yoon, T. Yabe, The unified simulation for incompressible and compressible flow by the predictor-corrector scheme based on the CIP method. Comput.Phys. Com. 119 (1999) 149.

[8] T.E. Tezduyar, J. Liou and D.K. Ganjoo, Incompressible flow computations based on the vorticity-stream function and velocity-pressure formulations, Computers & Structures 35 (1990) 445.